

# CD36 is a sensor of diacylglycerides

Kasper Hoebe<sup>1</sup>, Philippe Georgel<sup>1</sup>, Sophie Rutschmann<sup>1</sup>, Xin Du<sup>1</sup>, Suzanne Mudd<sup>1</sup>, Karine Crozat<sup>1</sup>, Sosathya Sovath<sup>1</sup>, Louis Shamel<sup>1</sup>, Thomas Hartung<sup>2</sup>, Ulrich Zähringer<sup>3</sup> & Bruce Beutler<sup>1</sup>

<sup>1</sup>Department of Immunology, The Scripps Research Institute, La Jolla, California 92037, USA

<sup>2</sup>EU Joint Research Centre, ECVAM, I-21020 Ispra, Italy

<sup>3</sup>Research Center Borstel, Leibniz-Center for Medicine and Biosciences, 23845 Borstel, Germany

Toll-like receptor 2 (TLR2) is required for the recognition of numerous molecular components of bacteria<sup>1–8</sup>, fungi<sup>9,10</sup> and protozoa<sup>11</sup>. The breadth of the ligand repertoire seems unusual, even if one considers that TLR2 may form heteromers with TLRs 1 and 6 (ref. 12), and it is likely that additional proteins serve as adapters for TLR2 activation. Here we show that an *N*-ethyl-*N*-nitrosourea-induced nonsense mutation of *Cd36* (*oblivious*) causes a recessive immunodeficiency phenotype in which macrophages are insensitive to the *R*-enantiomer of MALP-2 (a diacylated bacterial lipopeptide) and to lipoteichoic acid. Homozygous mice are hypersusceptible to *Staphylococcus aureus* infection. *Cd36<sup>obl</sup>* macrophages readily detect S-MALP-2, PAM<sub>2</sub>CSK<sub>4</sub>, PAM<sub>3</sub>CSK<sub>4</sub> and zymosan, revealing that some—but not all—TLR2 ligands are dependent on CD36. Already known as a receptor for endogenous molecules, CD36 is also a selective and nonredundant sensor of microbial diacylglycerides that signal via the TLR2/6 heterodimer.

In a G3 population of mice homozygous for *N*-ethyl-*N*-nitrosourea (ENU)-induced mutations<sup>13</sup>, we identified an animal that was hyporesponsive both to macrophage-activating lipopeptide 2 from *Mycoplasma pneumoniae* (MALP-2) and to a crude preparation of commercial peptidoglycan derived from *Staphylococcus aureus*. Biochemical analysis of the peptidoglycan preparation showed that the microbial inducer to which the mutant mouse was insensitive was lipoteichoic acid (LTA; Supplementary Fig. IS-1). Both MALP2 and LTA are TLR2/6-dependent microbial stimuli. However, macrophages from this mouse showed normal responses to the synthetic tri-acylated lipopeptide PAM<sub>3</sub>CSK<sub>4</sub> (a TLR1/2 ligand<sup>5,14</sup>) and zymosan (a TLR2/6 ligand<sup>12</sup>).

This mouse was bred to establish a homozygous stock on a pure C57BL/6 background. The phenotype was named *oblivious* to denote insensitivity to two TLR2 agonists that were both diacylglycerides. *Oblivious* behaved as a strictly recessive mutation (Fig. 1).

The molecular specificity of the sensing deficit in *oblivious* mice was further examined using synthetic *S*- and *R*- enantiomers of MALP-2 as well as diacylated and triacylated molecules with the peptide moiety -Cys-Ser-(Lys)<sub>4</sub> (Supplementary Fig. IS-2a–d). The tumour necrosis factor (TNF)-inducing activities of LTA, S-MALP-2 and R-MALP-2, PAM<sub>2</sub>CSK<sub>4</sub> and PAM<sub>3</sub>CSK<sub>4</sub> are each fully dependent on TLR2 (Supplementary Fig. IS-2e). However, only responses to R-MALP-2 and LTA were affected by the *oblivious* mutation. In addition, dose–response curves with LTA show that the inhibition observed for *oblivious* macrophages is not complete as observed for TLR2 knockout mice, suggesting that the *oblivious* gene product facilitates but is not absolutely required for LTA sensing (Supplementary Fig. IS-2f). Consistent with this finding was our observation of partial preservation of MyD88-dependent signal transduction events when either LTA or MALP-2 was used as an inducing stimulus in *oblivious* macrophages (Supplementary Fig. IS-3). It may be concluded that *oblivious*-assisted activation of TLR2 depends on the number of fatty acid groups that are present, the chirality, and the size and/or composition of the peptide group.

*Oblivious* homozygotes all develop an ocular pterygium by 6–12 months of age, apparently as the result of spontaneous colonization with *Corynebacterium* species and *Staphylococcus lentus*. On occasion, colonization progresses to spontaneous endophthalmitis (Supplementary Fig. IS-4). Luminescent *Staphylococcus aureus* was used as a direct test of the ability of *oblivious* mice to control an intradermal and/or intravenous Gram-positive inoculum. *Tlr2*-null and/or *Tirap*-null mice were taken as controls to assess the severity of the phenotype. During a 7-day period, *oblivious* and *Tlr2*<sup>-/-</sup> mice were permissive for the growth of intradermally inoculated *S. aureus*, whereas the bacteria were cleared in wild-type C57BL/6 mice (Fig. 2a). Survival of wild-type, *oblivious*, *Tlr2*<sup>-/-</sup> and *Tirap*<sup>-/-</sup> mice and bacterial growth was monitored during a 10-day period after challenge with 10<sup>8</sup> colony-forming units (c.f.u.) of *S. aureus* per mouse, administered intravenously. *Tlr2*<sup>-/-</sup> mice all succumbed to infection within 5 days. *Tirap*<sup>-/-</sup> and *oblivious* mice were less susceptible but accumulated more organisms during the course of infection, and died more frequently than wild-type mice (Fig. 2b, c). This is consistent with analyses of TNF production *in vitro* by peritoneal macrophages stimulated with LTA or MALP-2. *Tirap*<sup>-/-</sup> and *oblivious* cells showed a residual response, whereas *Tlr2*<sup>-/-</sup> cells were completely unresponsive (Fig. 2d). *In vitro*

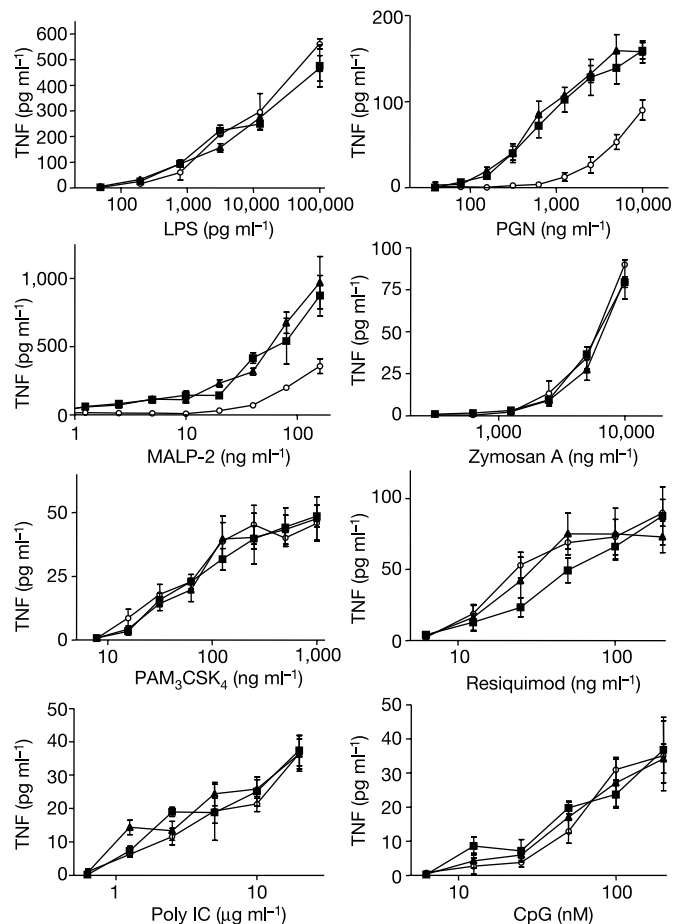


**Figure 1** *Oblivious* specifically reduces TNF production in response to *Staphylococcus*-derived peptidoglycan and synthetic MALP-2. Mice were injected with 3% thioglycollate; after 3 days, macrophages were cultured at a density of  $5 \times 10^5$  cells per well in 96-well plates. Wild-type (solid squares), *obl/+* (solid triangle) and *obl/obl* (open circle) macrophages were incubated with various concentrations of each specific inducer. After 4 h of incubation, supernatants were collected and assayed in duplicate for TNF activity as described previously<sup>24</sup>. Values are means  $\pm$  s.e.m. ( $n = 4$  mice).

responses to heat-killed *S. aureus* were similar, although the differences were less pronounced than observed for LTA or MALP2 (Fig. 2e).

The *oblivious* phenotype was mapped by outcrossing homozygotes to C3H/HeN mice and backcrossing the progeny to the mutant stock. On the basis of 28 meioses genotyped at 59 genome-wide microsatellite markers, *obl* was assigned to chromosome 5 (Fig. 3a). Further mapping on a total of 658 meioses permitted confinement to a 1.15-megabase chromosomal interval containing five genes (Fig. 3b, Supplementary Table 1). Sequencing revealed a point mutation (nucleotide 1022 T → A with respect to GenBank accession no. NM\_007643) in the distal coding region of *Cd36* (exon 11), creating an early stop codon and removing 133 residues from the carboxy terminus of the polypeptide chain, thereby preventing the formation of the second of two transmembrane domains represented in the normal protein (Fig. 3c–e). No mutations were identified within the other genes of the critical region, all of which were bidirectionally sequenced at complementary DNA or genomic levels.

We analysed CD36 expression on +/+, *obl*/+ and *obl/obl* macrophages using flow cytometry. *obl/obl* macrophages and platelets showed no expression of CD36 on the surface, whereas *obl*/+ macrophages showed reduced expression compared with +/+ macrophages (Fig. 4a, b). Western blot analysis with antibodies

directed against the amino-terminal part of CD36 showed an absence of CD36 in whole cell extracts as well as in supernatant (Supplementary Fig. IS-5). The phenotype observed for *CD36<sup>obl/obl</sup>* was identical to that observed in *CD36<sup>-/-</sup>* mice (Fig. 4c). Finally, *obl/obl* cells that were transfected with an expression vector encoding normal CD36 were capable of producing TNF in response to LTA (Fig. 4d). We therefore concluded that the *Cd36<sup>obl</sup>* mutation was solely responsible for the *oblivious* phenotype and that the *Cd36<sup>obl</sup>* allele is functionally equivalent to a null allele.

HEK-293 cells were transfected to express CD36, in combination with TLR2 and/or TLR6 and a nuclear factor (NF)-κB reporter gene. LTA and MALP-2 both caused NF-κB activation when cells were transfected to express TLR2, whereas transfection with plasmids encoding CD36 or TLR6 alone did not support activation by either ligand. The response to LTA and S-MALP was significantly augmented when either CD36 or TLR6 was coexpressed with TLR2. Coexpression of TLR2, TLR6 and CD36 gave the highest responses of all, indicating that CD36 does indeed facilitate the response to LTA and S-MALP, and does so best in the presence of TLR6, although neither TLR6 nor CD36 is absolutely required for a response (Supplementary Fig. IS-6).

CD36 is a member of the scavenger receptor type B family (Supplementary Fig. IS-7)<sup>15</sup>. It has been implicated in the recognition of oxidized LDL particles and the uptake of fatty acids<sup>16,17</sup>.

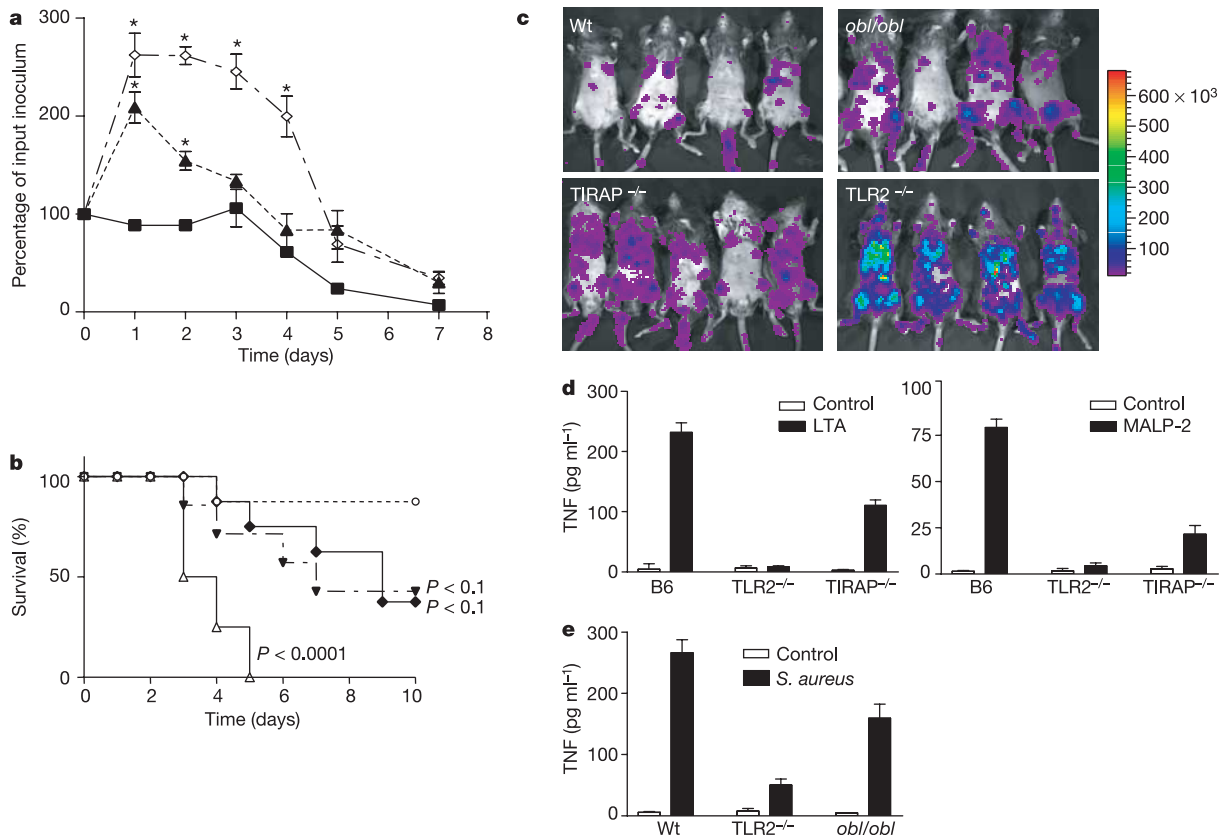


**Figure 2** *Oblivious* homozygous mutant mice are unable to contain Gram-positive *S. aureus* infections. **a**, Wild-type C57BL/6 male mice (filled squares), TLR2 knockout (open diamonds) and homozygous *oblivious* (filled triangles) mutant mice were each injected subcutaneously with *S. aureus* ( $10^5$  c.f.u. ml<sup>-1</sup>). During a 7-day period, bacterial growth was monitored daily with the Xenogen IVIS imaging system. Luminescence is depicted as a percentage of input, with 100% being the luminescence at day zero. Data are shown as means  $\pm$  s.e.m. ( $n = 6$ ). Asterisk,  $P < 0.001$  (compared with wild-type mice). **b**, Survival of wild-type C57BL/6 mice (open circles), *Tlr2*<sup>-/-</sup> (open triangles), *Tirap*<sup>-/-</sup> (filled triangles) and *obl/obl* (filled diamonds) mutant mice after intravenous

administration of *S. aureus* ( $10^8$  c.f.u. per mouse);  $n = 8$  for each group;  $P$  refers to comparison with C57BL/6. **c**, Luminescence in normal C57BL/6 (Wt), *Tlr2*<sup>-/-</sup>, *Tirap*<sup>-/-</sup> and *obl/obl* mutant mice at day 2 after intravenous injection with *S. aureus* ( $10^8$  c.f.u. ml<sup>-1</sup>). **d**, TNF production induced by LTA (left) and MALP-2 (right) in peritoneal macrophages derived from wild-type, *Tlr2*<sup>-/-</sup> and *Tirap*<sup>-/-</sup> mice during a 4-h incubation. **e**, TNF production induced by heat-killed *S. aureus* ( $10^6$  c.f.u. ml<sup>-1</sup>) in peritoneal macrophages derived from wild-type, *Tlr2*<sup>-/-</sup> and *obl/obl* mice during a 4-h incubation. Error bars represent s.e.m. of three independent experiments.

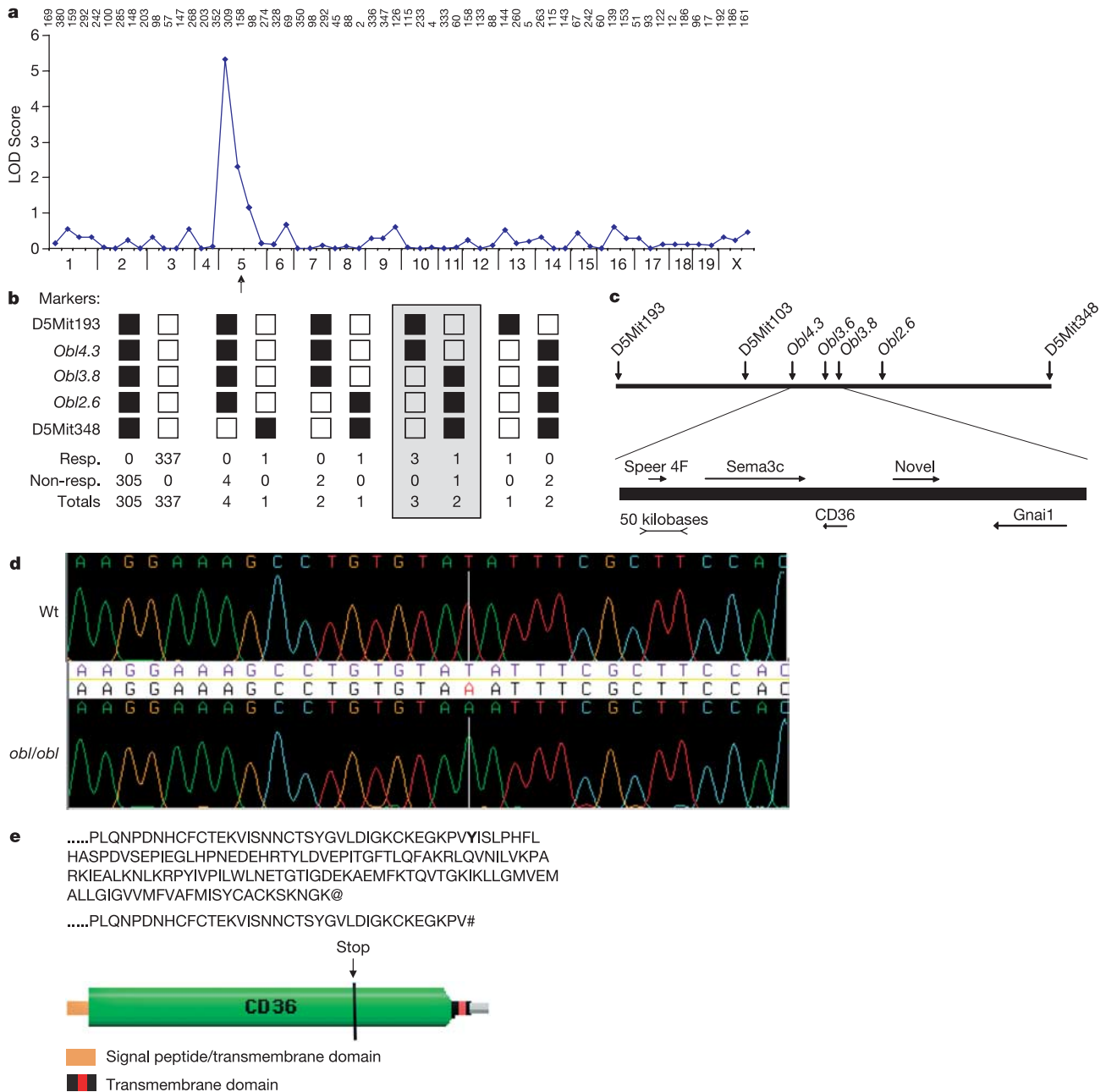


**Figure 3** Confinement of the *obl* critical region and identification of the *obl* mutation. **a**, Coarse genetic mapping of *oblivious*. Phenotypic classification of F<sub>2</sub> mice was based on a comparison of peptidoglycan-induced dose–response curves by measuring TNF production with the L929 bioassay. On 29 meioses, *obl* was confined to the proximal half of chromosome 5 with a peak LOD score of 5.3 associated with D5Mit352. **b**, On 658 meioses, the mutation was confined between novel polymorphic microsatellites *Obl4.3* and *Obl3.8* (shaded box; markers shown in Supplementary Table 1), and is separated from the limiting markers by four crossovers on the proximal site and one confirmed crossover on the distal side. Resp., ‘responder’ (to peptidoglycan); non-resp., ‘non-responder’; filled squares, homozygous; open squares, heterozygous. **c**, The critical

region is flanked by the public markers D5Mit193 and D5Mit348, and by the informative microsatellites shown in Supplementary Table 1. Within the critical region, a nominal listing of five genes is presented in the Ensembl database, with the arrangement and orientation shown. **d**, Consed display (<http://www.phrap.org/consed/consed.html>) of the mutation, showing the sequence from the distal coding region of a *Cd36<sup>obl/obl</sup>* homozygote (bottom trace) and from a normal C57BL/6 mouse (top trace). The mutation involves a single base transversion from T to A in the mutant strain, causing the nonsense substitution Y340#. **e**, The predicted sequence and graphical display of the Cd36 protein in normal (top) and mutant (bottom) mice.

However, no defined molecules of eubacterial origin have previously been shown to signal through CD36, nor has any function of CD36 previously been shown to be dependent on TLR. Our data suggest that CD36 acts as a facilitator or co-receptor for di-acylglyceride recognition through the TLR2/6 complex. Thus, CD36 serves a function analogous to CD14, which concentrates the lipopolysaccharide (LPS) signal for trans-

duction through TLR4 (ref. 18).

CD36 also has an established role in the recognition of endogenous ligands<sup>19</sup> and might therefore represent a signalling bridge between endogenous inducers and the principal innate immune sensors of the mammalian host. Potentially, such a bridge might be important in the pathogenesis of sterile inflammatory conditions. □

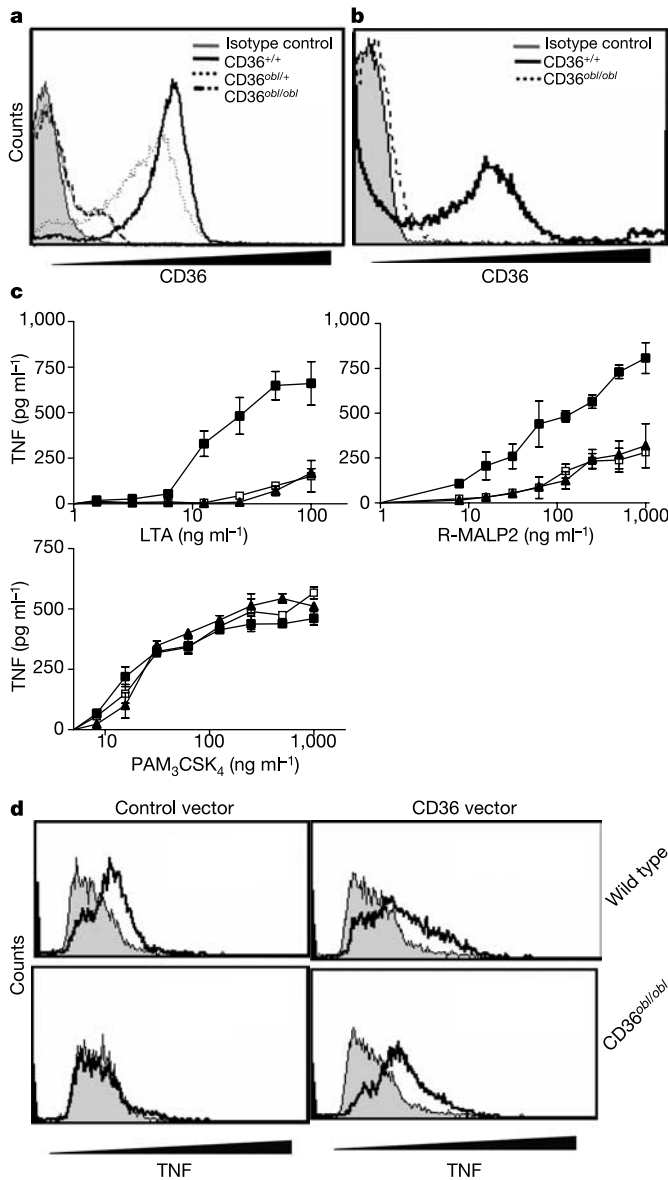


**Figure 4** A nonsense mutation in CD36 is responsible for the *oblivious* phenotype. **a, b**, Surface expression of CD36 on peritoneal macrophages (**a**) and platelets (**b**) derived from wild-type, *obl*<sup>+/+</sup> and/or *obl*<sup>obl/obl</sup> mice. Cells were labelled with a primary monoclonal antibody against mouse CD36 or with an isotype control, then exposed to a secondary anti-mouse IgA coupled to phycoerythrin. **c**, Comparison of peritoneal macrophage responses between wild-type (filled squares), *Cd36*<sup>-/-</sup> (filled triangles) and *Cd36*<sup>obl/obl</sup> (open squares) mice when exposed to LTA, R-MALP2 or PAM<sub>3</sub>CSK<sub>4</sub>. Error bars represent s.e.m. of three independent experiments. **d**, Rescue of the phenotype after co-transfection of bone-marrow-derived macrophages from normal or homozygous mutant mice with an expression vector encoding yellow fluorescent protein as well as an empty vector (control), or with a 1:3 mixture of expression vectors encoding yellow fluorescent protein and normal Cd36 as described before<sup>23</sup>. Untreated, shaded histogram; LTA (10 ng ml<sup>-1</sup>)-treated, unshaded histogram.

**Methods**

**Mice**

TLR2 knockout mice were provided by Tularik Inc., and Tirap knockout mice were obtained from R. Medzhitov (Yale University School of Medicine, New Haven, Connecticut). CD36 knockout mice were a gift from M. Febbraio (Cleveland Clinic Foundation, Cleveland, Ohio).

**Innate immune activators, probes and antibodies**

*Salmonella minnesota* Re595 LPS was obtained from Alexis. dsRNA was purchased from Amersham Pharmacia Biotech. Racemic MALP-2, S-MALP-2 and R-MALP-2, PAM<sub>3</sub>CSK<sub>4</sub>

and PAM<sub>2</sub>CSK<sub>4</sub> were obtained from EMC microcollections GmbH and peptidoglycan was purchased from Fluka. Phosphorothioate-stabilized CpG oligodeoxynucleotide (CpG-ODN) 5'-TCC-ATG-ACG-TTC-CTG-ATG-CT-3' was obtained from Integrated DNA Technologies. Phospho-specific antibodies for extracellular signal-related kinases (ERKs), p38, c-Jun N-terminal kinase (JNK) and antibodies against IκB were obtained from Cell Signalling Technology. Monoclonal antibodies against mouse CD36 (MAB1258) were obtained from Chemicon International and polyclonal antibodies against human CD36 were obtained from Cayman Chemical. Phycoerythrin-labelled anti-mouse IgA was purchased from E-Bioscience. Purified LTA was prepared as described previously<sup>6</sup>.

**Purification and analysis of the bioactive material in peptidoglycan**

Insoluble peptidoglycan (uPG) was prepared from *Staphylococcus aureus* and residual teichoic acid was removed as described<sup>20</sup>. Chloroform/methanol extraction of this uPG preparation revealed bioactivity in the organic phase, strongly implicating lipids rather than PG as the CD36 ligand(s). Further purification of these lipids by silica-gel chromatography and subsequent analysis of bioactive fractions by mass spectrometry revealed several lipophilic partial structures of LTA, including gentiobioside-diaclylglycerol (the LTA lipid anchor)<sup>21</sup> carrying one glycerol phosphate unit (Gro-P-β-D-Glcp-(1 → 6)-β-D-Glcp-DAG, where Gro stands for glycerol, Glc for glucosyl, p for phospho, and DAG for diacylglycerol).

**Western blotting**

Western blot analysis of JNK, p38, STAT and ERK1/2 phosphorylation, and degradation of IκB was performed as described previously<sup>22</sup>. For western blot analysis of CD36 in cell extracts or supernatants, anti-(human CD36) polyclonal antibodies showing crossreactivity to mouse CD36 were used. For analysis of supernatants, macrophages were incubated for 24 h in a small volume of medium and without the addition of fetal bovine serum.

**Rescue studies**

Rescue studies with bone marrow cells were performed as described previously<sup>23</sup>.

**Transfection of HEK-293 cells**

Cells were cultured in 96-well plates at a density of 2.5 × 10<sup>4</sup> cells per well and incubated overnight at 37 °C and 5% CO<sub>2</sub>. Cells were transfected overnight with NF-κB luciferase reporter gene (50 ng per well) and co-transfected with CD36, TLR2 and/or TLR6 (100 ng per vector per well; final concentration 350 ng per well). After stimulation for 5 h with various concentrations of LTA, S-MALP and PAM<sub>3</sub>CSK<sub>4</sub>, cells were lysed and luciferase activity was measured with a luciferase assay reagent (Promega).

**Germline mutagenesis**

ENU was obtained from Sigma. ENU germline mutagenesis was performed as described previously<sup>23</sup>. After identification of the *oblivious* mutant in the G3 macrophage screen, the founder was backcrossed to C57BL/6 mice to obtain further genetic purity.

**DNA sequencing**

Genes residing in the critical region were amplified by using primers chosen after masking with RepeatMasker. Fragments were sequenced bidirectionally with internal primers. Primers were obtained from Genosys.

**Infection with *Staphylococcus aureus***

Hair was removed by chemical depilation and the mice were injected subcutaneously with 100 μl of a mid-exponential growth phase (*D*<sub>600</sub> = 0.6, 5 × 10<sup>6</sup> c.f.u. ml<sup>-1</sup>) of *S. aureus* (Xen 8.1; parental strain 3825-4) resuspended in PBS and complexed to Cytodex beads (Sigma) as a carrier. During a 4-day period, bacterial growth was monitored daily with the Xenogen IVIS imaging system. In addition, in a separate experiment mice were administered 10<sup>8</sup> *S. aureus* intravenously without the use of Cytodex beads and were monitored for survival and bacterial growth during a 10-day period.

Received 1 November; accepted 3 December 2004; doi:10.1038/nature03253.

- Lien, E. *et al.* Toll-like receptor 2 functions as a pattern recognition receptor for diverse bacterial products. *J. Biol. Chem.* **274**, 33419–33425 (1999).
- Takeuchi, O. *et al.* Differential roles of TLR2 and TLR4 in recognition of Gram-negative and Gram-positive bacterial cell wall components. *Immunity* **11**, 443–451 (1999).
- Means, T. K. *et al.* Human toll-like receptors mediate cellular activation by *Mycobacterium tuberculosis*. *J. Immunol.* **163**, 3920–3927 (1999).
- Takeuchi, O. *et al.* Discrimination of bacterial lipoproteins by Toll-like receptor 6. *Int. Immunol.* **13**, 933–940 (2001).
- Takeuchi, O. *et al.* Cutting edge: role of Toll-like receptor 1 in mediating immune response to microbial lipoproteins. *J. Immunol.* **169**, 10–14 (2002).
- Morath, S., Stadelmaier, A., Geyer, A., Schmidt, R. R. & Hartung, T. Synthetic lipoteichoic acid from *Staphylococcus aureus* is a potent stimulus of cytokine release. *J. Exp. Med.* **195**, 1635–1640 (2002).
- Opitz, B. *et al.* Toll-like receptor-2 mediates *Treponema glycolipid* and lipoteichoic acid-induced NF-κB translocation. *J. Biol. Chem.* **276**, 22041–22047 (2001).
- Werts, C. *et al.* Leptospiral lipopolysaccharide activates cells through a TLR2-dependent mechanism. *Nature Immunol.* **2**, 346–352 (2001).
- Gantner, B. N., Simmons, R. M., Canavera, S. J., Akira, S. & Underhill, D. M. Collaborative induction of inflammatory responses by dectin-1 and Toll-like receptor 2. *J. Exp. Med.* **197**, 1107–1117 (2003).
- Brown, G. D. *et al.* Dectin-1 mediates the biological effects of β-glucans. *J. Exp. Med.* **197**, 1119–1124 (2003).
- Campos, M. A. *et al.* Activation of Toll-like receptor-2 by glycosylphosphatidylinositol anchors from a protozoan parasite. *J. Immunol.* **167**, 416–423 (2001).
- Ozinsky, A. *et al.* The repertoire for pattern recognition of pathogens by the innate immune system is defined by cooperation between Toll-like receptors. *Proc. Natl Acad. Sci. USA* **97**, 13766–13771 (2000).
- Hoeb, K. *et al.* Identification of Lps2 as a key transducer of MyD88-independent TIR signaling.

Nature 424, 743–748 (2003).

14. Morr, M., Takeuchi, O., Akira, S., Simon, M. M. & Muhlrad, P. F. Differential recognition of structural details of bacterial lipopeptides by Toll-like receptors. *Eur. J. Immunol.* **32**, 3337–3347 (2002).
15. Calvo, D., Dopazo, J. & Vega, M. A. The CD36, CLA-1 (CD36L1), and LIMP-II (CD36L2) gene family: cellular distribution, chromosomal location, and genetic evolution. *Genomics* **25**, 100–106 (1995).
16. Aitman, T. J. *et al.* Identification of Cd36 (Fat) as an insulin-resistance gene causing defective fatty acid and glucose metabolism in hypertensive rats. *Nature Genet.* **21**, 76–83 (1999).
17. Glazier, A. M., Scott, J. & Aitman, T. J. Molecular basis of the Cd36 chromosomal deletion underlying SHR defects in insulin action and fatty acid metabolism. *Mamm. Genome* **13**, 108–113 (2002).
18. Wright, S. D., Ramos, R. A., Tobias, P. S., Ulevitch, R. J. & Mathison, J. C. CD14, a receptor for complexes of lipopolysaccharide (LPS) and LPS binding protein. *Science* **249**, 1431–1433 (1990).
19. Gordon, S. Pattern recognition receptors: doubling up for the innate immune response. *Cell* **111**, 927–930 (2002).
20. Rosenthal, R. S. & Dziarski, R. Isolation of peptidoglycan and soluble peptidoglycan fragments. *Methods Enzymol.* **235**, 253–285 (1994).
21. Deisinger, S. *et al.* Definition of structural prerequisites for lipoteichoic acid-inducible cytokine induction by synthetic derivatives. *J. Immunol.* **170**, 4134–4138 (2003).
22. Kim, S. O., Ono, K. & Han, J. Apoptosis by pan-caspase inhibitors in lipopolysaccharide-activated macrophages. *Am. J. Physiol. Lung Cell. Mol. Physiol.* **281**, L1095–L1105 (2001).
23. Hoebe, K., Du, X., Goode, J., Mann, N. & Beutler, B. *Lps2*: a new locus required for responses to lipopolysaccharide, revealed by germline mutagenesis and phenotypic screening. *J. Endotoxin Res.* **9**, 250–255 (2003).
24. Poltorak, A. *et al.* Genetic and physical mapping of the *Lps* locus—identification of the toll-4 receptor as a candidate gene in the critical region. *Blood Cells Mol. Dis.* **24**, 340–355 (1998).

**Supplementary Information** accompanies the paper on [www.nature.com/nature](http://www.nature.com/nature).

**Acknowledgements** This work was supported by the NIH.

**Competing interests statement** The authors declare that they have no competing financial interests.

**Correspondence** and requests for materials should be addressed to B.B. ([bruce@scripps.edu](mailto:bruce@scripps.edu)).

## Plastid proteins crucial for symbiotic fungal and bacterial entry into plant roots

Haruko Imaizumi-Anraku<sup>1,2,\*</sup>, Naoya Takeda<sup>3,\*</sup>, Myriam Charpentier<sup>4,†</sup>, Jillian Perry<sup>4</sup>, Hiroki Miwa<sup>5</sup>, Yosuke Umehara<sup>1,6</sup>, Hiroshi Kouchi<sup>1,6</sup>, Yasuhiro Murakami<sup>1,2</sup>, Lonneke Mulder<sup>4</sup>, Kate Vickers<sup>4</sup>, Jodie Pike<sup>4</sup>, J. Allan Downie<sup>5</sup>, Trevor Wang<sup>5</sup>, Shusei Sato<sup>7</sup>, Erika Asamizu<sup>7</sup>, Satoshi Tabata<sup>7</sup>, Makoto Yoshikawa<sup>3</sup>, Yoshikatsu Murooka<sup>3</sup>, Guo-Jiang Wu<sup>8</sup>, Masayoshi Kawaguchi<sup>6,8</sup>, Shinji Kawasaki<sup>1,2</sup>, Martin Parniske<sup>4,†</sup> & Makoto Hayashi<sup>3,6</sup>

<sup>1</sup>National Institute of Agrobiological Sciences, 2-1-2 Kannondai, Tsukuba, Ibaraki 305-8602, Japan

<sup>2</sup>Bio-oriented Technology Research Advancement Institution (BRAINI), Tokyo Office, 3-18-19 Toranomon Minato-ku, Tokyo 105-0001, Japan

<sup>3</sup>Department of Biotechnology, Graduate School of Engineering, Osaka University, 2-1 Yamadaoka, Suita, Osaka 565-0871, Japan

<sup>4</sup>The Sainsbury Laboratory, John Innes Centre, Colney Lane, Norwich NR4 7UH, UK

<sup>5</sup>John Innes Centre, Colney Lane, Norwich NR4 7UH, UK

<sup>6</sup>Core Research for Evolutional Science and Technology (CREST), Japan Science and Technology Agency, 4-1-8 Honcho, Kawaguchi, Saitama 332-0112, Japan

<sup>7</sup>Kazusa DNA Research Institute, 2-6-7 Kazusa-kamatari, Kisarazu, Chiba 292-0818, Japan

<sup>8</sup>Department of Biological Sciences, Graduate School of Science, The University of Tokyo, 7-3-1 Hongo, Bunkyo, Tokyo 113-0033, Japan

\* These authors contributed equally to this work

† Present address: Genetics Institute, Ludwig Maximilians Universität (LMU), Maria-Ward-Str. 1a, D-80638 München, Germany

**The roots of most higher plants form arbuscular mycorrhiza, an ancient, phosphate-acquiring symbiosis with fungi, whereas only four related plant orders are able to engage in the evolutionary younger nitrogen-fixing root-nodule symbiosis with bacteria<sup>1</sup>. Plant symbioses with bacteria and fungi require a set of common**

signal transduction components that redirect root cell development<sup>2,3</sup>. Here we present two highly homologous genes from *Lotus japonicus*, *CASTOR* and *POLLUX*, that are indispensable for microbial admission into plant cells and act upstream of intracellular calcium spiking<sup>4</sup>, one of the earliest plant responses to symbiotic stimulation. Surprisingly, both twin proteins are localized in the plastids of root cells, indicating a previously unrecognized role of this ancient endosymbiont in controlling intracellular symbioses that evolved more recently.

Upon recognition of a bacterial symbiotic signalling molecule, the ‘Nod factor’, root hairs of leguminous plants reprogramme their development<sup>5,6</sup>. Tip growth is redirected to form a curl that entraps a bacterial microcolony to initiate the formation of the infection thread. These events are preceded by the rapid formation of transient subcellular gradients of proton, potassium, chloride and calcium ions, followed after about 10 min by oscillations in intracellular calcium concentration, the ‘calcium spiking’ response<sup>7</sup>. We used *Lotus japonicus* mutants to identify the molecular players of this electrochemical prelude to symbiosis. Mutants affected in the *CASTOR* or *POLLUX* genes exhibit very similar phenotypes; they do not form root nodules or arbuscular mycorrhizal symbiosis. Root hairs treated with *Mesorhizobium loti* or Nod factor show branching and tip swelling (Fig. 1a–f, and data not shown), but infection threads are never formed. Similarly, in the arbuscular mycorrhizal symbiosis, fungal entry into root epidermal cells is not supported, and infection attempts are aborted<sup>8–11</sup>. Root hairs of all tested *castor*<sup>12</sup> and *pollux* mutants lacked the Nod-factor-induced calcium spiking that is typically seen with wild-type (Fig. 1g). However, root-hair branching was observed in these non-spiking mutants (Fig. 1e, f) and so some of the earliest plant responses to Nod factors can be genetically uncoupled. These results demonstrate that *CASTOR* and *POLLUX* act very early in a signal transduction chain leading from the perception of Nod factor to the activation of calcium spiking. They are also required for the execution of the appropriate morphological response of the root hair, because only branching and deformation, but not curling or infection thread formation, were observed.

The *CASTOR* and *POLLUX* genes were isolated through positional cloning and by their strong sequence similarity. Using the extensive collection of microsatellite (simple sequence repeat (SSR)) markers available for *L. japonicus*<sup>13</sup>, the *CASTOR* and *POLLUX* genes were positioned close to the bottom ends of chromosomes 1 and 6, respectively. Analysis of the sequence obtained in the context of the genome project<sup>14</sup> revealed very limited local similarity between the *CASTOR* and *POLLUX* genomic regions. Only *CASTOR* and *POLLUX* themselves were conserved, suggesting that the two genes are the product of a limited duplication event (Supplementary Fig. 1).

Five *castor* alleles were independently mapped to the south end of chromosome 1, close to SSR marker TM0105 (ref. 14). Starting with this marker, a bacterial artificial chromosome (BAC)<sup>15</sup>/transformation-competent artificial chromosome (TAC)<sup>14</sup> contig (Supplementary Fig. 1b) was constructed that extended into the telomeric region, as indicated by multiple copies of subtelomeric repeat LjTR4 (M.H., unpublished data) towards the southern extremity (Supplementary Fig. 1b). Genetic mapping was affected by an inversion 145 kilobases (kb) long between the parental lines B-129 and MG-20 (ref. 16) with no recombination events observed on inspection of 1,833 individuals of five different F<sub>2</sub> populations (Supplementary Fig. 1a), delimiting the *CASTOR* locus to a region of about 240 kb. Polymerase chain reaction (PCR) marker TB2R could not be amplified from individuals homozygous for the *castor-8* or *castor-9* alleles. PCR and Southern blot analysis (Fig. 2a) indicated that both alleles have large deletions of more than 20 kb encompassing the *CASTOR* gene, and subsequent sequence analysis revealed that marker TB2R is located in a *CASTOR* intron (Supplementary Fig. 1d).

Sequencing of genomic DNA identified non-silent mutations within the *CASTOR* gene in 15 additional mutants, thus providing a